A Numerical Investigation of the Effect of Spatial and Temporal Resolution together with Turbulence Modelling on the Hydrodynamic Forces of a Cavitating Foil

Mariana ZAMMIT MUNRO [a,1] , Simon MIZZI [b],
Claire DE MARCO MUSCAT FENECH [c], Giorgio TANI [d], Yigit DEMIREL[e]
[a,b,c] *University of Malta*
[d] *Universita' degli Studi di Genova*
[e] *University of Strathclyde*

Abstract. Cavitation is a highly destructive phenomenon that significantly disrupts the performance of propellers and control surfaces in the maritime industry. Hence, the prediction of forces developed during cavitation, through various numerical techniques, is imperative for the design and operation of maritime vessels.

RANS turbulence models have proven to be the most computationally viable option for such a fast-paced industry. The work presented here analyses and compares several of these well-established models, including the SST k-ω and k-ε RNG models modified to account for compressibility effects.

This paper aims to provide insight into the influence of timestep, mesh resolution and turbulence model on the hydrodynamic forces acting on a 2D cavitating hydrofoil, so as to facilitate future simulations.

Keywords. Cavitation, CFD, RANS, turbulence modelling

1. Introduction

Cloud cavitation is one of the most damaging forms of cavitation as it is unstable and generates intense vibration and noise. The turbulent and unsteady nature of cavitating flows renders it more difficult to simulate numerically. To date, several authors have produced promising results in the simulation of unsteady, turbulent cavitating flows around hydrofoils using Computational Fluid Dynamics (CFD) software. For instance, Bensow [1] employed different turbulence closure approaches to simulate unsteady cavitation on the Delft Twist11 foil: Large Eddy Simulation (LES), Detached Eddy Simulation (DES) and Unsteady Reynolds Averaged Navier-Stokes (URANS).

For the URANS approach, the Spalart-Allmaras turbulence model was chosen, with and without the Reboud correction [2], which reduces the turbulent viscosity in the mixture region with the purpose of accounting for compressibility effects. Bensow [1] found that LES produced the most accurate results with regard to shedding frequency, but that the result of the lift coefficient (C_L) was underpredicted for all approaches. However, LES requires a relatively dense grid resolution in comparison to URANS, and hence the latter tends to be preferred for its computational efficiency.

[1] Corresponding author, Mechanical Engineering Department, University of Malta, Msida, MSD 2080, Malta; E-mail: mariana.zammit-munro.16@um.edu.mt

The results of the URANS simulation without the Reboud correction predicted a steady cavity behaviour without shedding, whereas all other turbulence model approaches produced unsteady, cloud cavitation with large shedding [1]. The inability to predict cavity shedding by the traditional URANS models has been observed by many authors and the Reboud correction has been widely recognised as being able to produce accurate unsteady cavitation behaviour ([3], [4], [5], [6]). The most frequently selected URANS turbulence models for the simulation of unsteady cavitation, whether in a Venturi or around a hydrofoil, are the SST k-ω and k-ε RNG models. Goncalves da Silva [7] simulated unsteady cavitation in a Venturi and found the SST k-ω model to best reproduce the experimental observations. Both Leroux et al. [3] and Zhou and Wang [5] employed the modified k-ε RNG turbulence model (with standard wall functions) to simulate unsteady cavitation over a NACA66(mod) hydrofoil and found that the unsteadiness of the experimental data was well reproduced.

The temporal resolution of cavitation simulations is another topic of interest that requires further investigation. Different methods for selecting a suitable timestep for unsteady cavitation simulations have been adopted in the literature. Table 1 gives a summary of the timesteps employed by various authors who simulated unsteady cavitation. The timesteps presented in italic are those chosen by the authors following their timestep study, which were deemed accurate enough to apply to the main analysis.

Coutier-Delgosha et al. [6] computed the timestep of their unsteady cavitation simulation in a Venturi using the reference time, T_{ref}, which was a function of the chord length and inlet flow velocity, and multiplied it by three factors: 0.01, 0.005 and 0.002. Although the shedding frequency obtained at the finest timestep resulted in the lowest error when compared to the experimentally measured value, Coutier-Delgosha et al. [6] suggest that the influence of the timestep cannot be completely removed. Moreover, the use of a second-order time integration scheme did not have a significant effect on the results obtained.

Table 1. Timesteps employed by various authors investigating unsteady cavitation

Authors	**Coutier-Delgosha et al.** [6]	**Leroux et al.** [3]	**Zhang et al.** [8]	**Zhou and Wang** [5]	**Geng and Escaler** [4]	**Lindau et al.** [9]
Timestep (x 10^{-5} s)	31.94	14.07	50.00	100.00	*5.00*	*500.00*
	15.97		*10.00*	*50.00*	2.00	250.00
	6.39		5.00	10.00		*100.00*

Leroux et al. [3] studied unsteady cloud cavitation around a two-dimensional NACA66(mod) hydrofoil and for their numerical analysis also employed the concept of a reference time, T_{ref}. Similarly, Zhang et al. [8] and Zhou and Wang [5] analysed the experimental case of Leroux et al. [10] and carried out a temporal convergence study to determine the effect of timestep size on pressure fluctuation. While there was a significant difference in the calculated pressure fluctuation between the coarsest and in-between timesteps, Zhang et al. [8] noted a very slight difference between the latter and the finest timesteps. Although no comparison was given by the Zhou and Wang [5] in the paper, it was stated that the three timesteps were found to obtain similar results. In the timestep study conducted by Lindau et al. [9], the coarsest and finest timesteps obtained the same result for cavity cycling frequency when investigating unsteady cavitation around an axisymmetric cavitator.

Geng and Escaler [4] investigated the influence of empirical coefficients F_v and F_c in the Zwart cavitation model by analysing the development of unsteady cloud cavitation around a two-dimensional NACA65012 hydrofoil. It is noted that use of the

finer timestep resulted in a calculated frequency with a greater error when compared to the measured frequency. However, the comparison of just two timesteps cannot provide sufficient insight into the issue of solution convergence in the temporal domain, so further analysis is required.

The purpose of the present work is to address the gap in the literature regarding the influence of timestep, mesh size and turbulence model on the simulation of unsteady, turbulent cavitating flow. Additionally, the influence of the Zwart cavitation model empirical coefficients, F_v and F_c, on the hydrodynamic coefficients, instantaneous pressure and shedding frequency is evaluated. Two URANS turbulence model approaches, modified with the Reboud correction, will be examined in this analysis.

2. Experimental Case and Numerical Approach

2.1. Experimental Case

The experimental case investigated by Leroux et al. [10] has been used for this analysis. For the study, a NACA66(mod) two-dimensional hydrofoil of chord length c 0.150 m and span s 0.191 m was used. The test section was 1 m long with a square cross-section of side 0.192 m. Pressure transducers were positioned on the foil suction side to measure the instantaneous pressure at nine positions along the chord, from chord ratios 0.1 to 0.9. The inlet reference velocity V_{ref} into the test section was 5.33 m/s and the Reynolds number based on the chord length was 0.8 x 10^6. The angle of attack was set to 6° and the cavitation number was kept constant at $\sigma = (P_{in} - P_V)/(0.5\rho_l V_{ref}^2) = 1$ by adjusting the inlet pressure. The temperature during the experiment was 20°C.

Leroux et al. [10] noted the development of unsteady cloud cavitation with a shedding frequency f of 3.625 Hz, resulting in a Strouhal number based on chord length, $St = fc/V_{ref} = 0.102$. The experimental results relating to the instantaneous pressure and frequency have been chosen for validation of the present study.

2.2. Numerical Approach

To model the turbulent cavitating flow, the Volume of Fluid (VOF) multiphase model with implicit formulation was adopted, which tracks the volume fraction of each phase throughout the domain. The model assumes an incompressible single-fluid approach, where the different phases share the same pressure and velocity fields and there is no slip velocity between them.

The vapour volume fraction, α_v, is defined as the ratio of the vapour volume to total cell volume and is determined from Eq. (1). Generally, the mass transfer rate calculation is carried out using a cavitation model that is based on a simplified form of the Rayleigh-Plesset equation which ignores viscosity, surface tension, thermodynamic and non-condensable gas effects, as described in Eq. (2). In this analysis, the Zwart cavitation model described in Eqs. (3) and (4) has been employed, which assumes the vapour bubble radius R_B and nucleation site volume fraction α_{nuc} to be constant. In Eqs. (1) to (4), u is the mixture flow velocity, ρ is the density, t is time, P_V is the saturated water vapour pressure, P_∞ is the pressure at infinity and R_e and R_c represent the evaporation and condensation source terms that account for the mass transfer rate between the water and vapour phases. The subscripts l and v denote the properties of the liquid and vapour

phases, respectively. F_v and F_c are case-dependent empirical coefficients for vaporisation and condensation, respectively, which should be tuned according to the cavitation regime and hydrodynamic conditions [4]. The default Zwart cavitation model constants are R_B = 1 x 10^{-6} m, α_{nuc} = 5 x 10^{-4} m, F_v = 50 and F_c = 0.01.

$$\frac{\partial(\alpha_v \rho_v)}{\partial t} + \nabla.(\alpha_v \rho_v u) = R_e - R_c \tag{1}$$

$$\frac{dR}{dt} = \sqrt{\frac{\frac{2}{3}(P_V - P_\infty)}{\rho_l}} \tag{2}$$

$$R_e = \frac{F_v(3\alpha_{nuc}(1-\alpha_v)\rho_v)}{R_B}\sqrt{\frac{\frac{2}{3}(P_V - P_\infty)}{\rho_l}} \qquad (P \le P_V) \tag{3}$$

$$R_c = \frac{F_c(3\alpha_v \rho_v)}{R_B}\sqrt{\frac{\frac{2}{3}(P_\infty - P_V)}{\rho_l}} \qquad (P \ge P_V) \tag{4}$$

The two URANS turbulence model approaches used to calculate the turbulent eddy viscosity μ_t in the analysis were the SST k-ω and k-ε RNG models. The compressibility effects of the mixture were accounted for by employing the Reboud correction, given in Eq. (5). The exponent *n* was set to a value of 10, as suggested by several authors [[2], [3], [6]] who successfully reproduced the cloud shedding process. User Defined Functions (UDFs) were compiled to modify the turbulent viscosity equations of both the SST k-ω and k-ε RNG models according to the Reboud correction, as given in Eqs. (6) and (7), respectively:

$$f(\rho) = \rho_v + \left(\frac{\rho_v - \rho_m}{\rho_v - \rho_l}\right)^n (\rho_l - \rho_v) \tag{5}$$

$$\mu_t = \frac{f(\rho) a_1 k}{\max(a_1 \omega, SF_2)} \tag{6}$$

$$\mu_t = \frac{f(\rho) c_\mu k^2}{\varepsilon} \tag{7}$$

where *k* is the turbulent kinetic energy, ω is the turbulent frequency, ε is the rate of dissipation of kinetic energy, c_μ = 0.085 for the RNG model, a_1 = 0.31, F_2 is a function of the cell distance from a wall and *S* is the strain rate magnitude. The pressure-velocity coupling is solved using the SIMPLE algorithm and the PRESTO scheme was used for the pressure interpolation. A first-order implicit time integration scheme was applied.

The computational domain represents the test section used in the experimental campaign by Leroux et al. [10] and was simplified to a 2D problem. The hydrofoil leading edge was placed 0.3c from the velocity inlet, at which a turbulent intensity of 1% was applied. The outlet condition was set to pressure outlet and the no-slip wall condition was applied to all other edges.

The SST k-ω and k-ε RNG models were chosen for this study because they are by far the most widely validated URANS turbulence models used for unsteady cavitation analysis. Although the k-ε models may be used as near-wall models, it was decided to use the k-ε RNG model with standard wall functions for this study, for more accurate comparison with similar numerical papers that also used Leroux et al.'s [10] experimental case [[3], [5], [8]] and who employed this turbulence model approach.

3. Mesh and Timestep Convergence Study

3.1. Mesh Convergence Study

The mesh requirements for the different turbulence models differ according to the wall treatment; therefore, separate meshes for the two turbulence models were created. The nondimensional wall distance y^+ is defined using Eq. (8), where τ_w is the wall shear stress, v is kinematic viscosity and y is the distance from the wall to the centre of the first cell.

$$y^+ = \frac{\sqrt{\left(\frac{\tau_w}{\rho}\right)}y}{v} \tag{8}$$

Meshes 1 and 2 were created such that the first cell centroid was positioned approximately at y^+ values of 1 and 30, for the SST k-ω and k-ε RNG turbulence models, respectively. Therefore, two mesh convergence studies were carried out to determine the optimal number of cells with regard to the accuracy of the results as well as computational time. According to the Grid Convergence Index Method (GCI) [11], three meshes were tested for each turbulence model, with a grid refinement factor $r = \sqrt{2}$. The GCI values of time-averaged total vapour volume V_{cav} for Meshes 1 and 2 are given in Table 2, which show that the results are within the asymptotic range, leading to the decision to use meshes M1.2 and M2.2 for the analysis. The timestep used for the mesh study was calculated according to the study by Coutier-Delgosha et al.[6]where a representative time T_{ref} was employed to determine the timestep size by means of the equation $\Delta t = 0.005T_{ref}$. Hence, using $T_{ref} = L_{ref}/V_{ref}$, where the chord length $L_{ref} = 0.15\ m$ and the inlet flow velocity $V_{ref} = 5.33\ m/s$, the resulting timestep was Δt =1.407 x 10^{-4} s.

Table 2. GCI Values and Number of Cells for the Mesh Convergence Study

Turbulence model	**Mesh number**	**Number of cells**	V_{cav} (x10^3 m^3)	**GCI (%)**	
	M1.1	70 000	0.125	GCI_{21} =	0.019
SST k-ω	M1.2	35 000	0.124	GCI_{32} =	0.534
	M1.3	17 500	0.110		
	M2.1	57 366	0.122	GCI_{21} =	0.066
k-ε RNG	M2.2	28 628	0.120	GCI_{32} =	1.564
	M2.3	14 535	0.154		

3.2. Timestep Convergence Study

A timestep convergence study for all meshes was carried out to determine which timestep would be suitable for the empirical coefficient study. The five timesteps analysed ranged from 2Δt to $\Delta t/8$, and the graphs of time-averaged C_L and V_{cav} against Timestep for M1.2 and M2.2 are displayed in Figure 1. The results show that the SST k-ω model predicts smaller and slightly more stable values of C_L and V_{cav} compared to the k-ε RNG model. The timestep chosen for the empirical coefficient study was $\Delta t/2$ since overall, it was the timestep that produced the most consistent results with regard to instantaneous pressure, V_{cav} and f for both models. However, in contrast to the mesh study, there is no noticeable trend with regard to the change in C_L or V_{cav} with timestep size, and no obvious monotonous convergence may be noted for any of the three meshes, similarly reported by Lindau et al. [9].

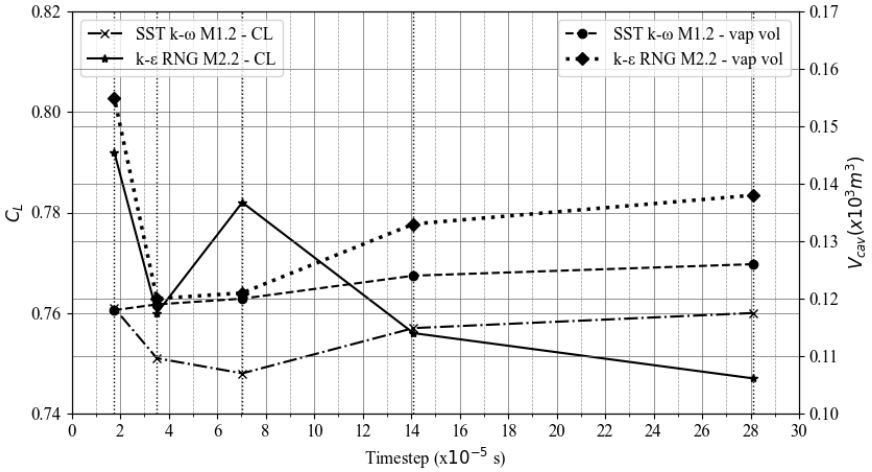

Figure 1. Graph of C_L against Timestep (x10^{-5} s) for both turbulence models for meshes M1.2 and M2.2

4. Comparison to Experimental Results

The cycle predicted by CFD is characterised by quasi-periodic cloud shedding approximately every 0.17 s, while in the experiment the period observed was around 0.276 s. Both turbulence models predict large cloud shedding, as is illustrated in Figure 2, which depicts the cycle for each model in comparison with photographs taken during the experiment [10]. The SST k-ω model simulates a slightly longer cycle (0.177 s) than the k-ε RNG model (0.127 s), but the time-averaged pressure for both models are very similar, resulting in a difference of only 2%. While the SST k-ω model produces more periodic peaks for V_{cav}, the time-averaged mean values calculated by both models are comparable, with a difference of only 3% between them.

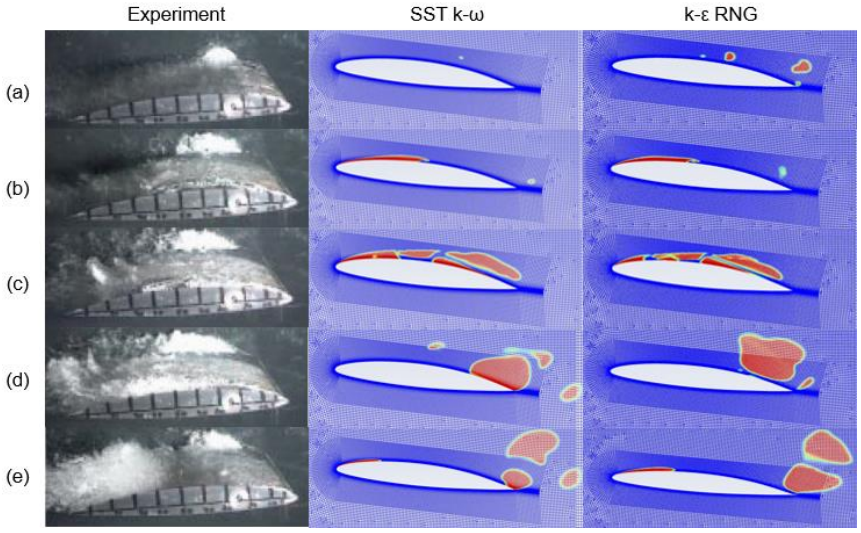

Figure 2. Vapour volume fraction contour plots for the SST k-ω and k-ε RNG turbulence models

Compared to the experiment by Leroux et al. [10], higher pressure peaks are predicted by both turbulence models but cavity length is accurately simulated with maximum values of 0.75 c to 0.8 c. Cavity lengths of 0.75 c for this cavitation regime were also reported by Shen and Dimotakis [12], who conducted experiments on an identical hydrofoil under the same conditions, except for the higher Reynolds number of 2×10^6 as opposed to the simulation Reynolds number of 0.8×10^6. Moreover, numerical analysis conducted by Leroux et al. [3] and Zhou and Wang [5] produced cavity lengths from 0.7 c to 0.8 c. As portrayed in Figure 2(a), a pressure peak pre-empts a sudden decrease in vapour volume content, and represents the start of a new cycle, which is also described by Leroux et al. [3] and Zhou and Wang [5].

With regard to the hydrodynamic forces acting on the foil, the simulations predict an increase in C_L as the cavity grows, which reaches its maximum at cloud detachment and consequently decreases as the cavity collapses. The analysed behaviour is noted in the numerical calculations [[3], [5]] and is also in line with the experimental observations by Shen and Dimotakis [12], who recorded a significant increase in the measured lift and drag forces when the foil experienced partial cavitation with cavity lengths up to 0.8 c.

5. Empirical Coefficient Study

For the study of the Zwart cavitation model empirical coefficients F_v and F_c, a parametric analysis which comprised of 50 computational runs was carried out. The total time of the simulations was selected to be $20T_{ref}$, as suggested by Coutier-Delgosha et al. [6]. Both turbulence models were tested with a range of five F_v and F_c values, from 50 to 450 and 0.01 to 0.09, respectively. The results chosen for comparison were drag coefficient C_D, C_L, V_{cav}, and the instantaneous pressure along the chord as conducted in the experiment. The frequency was calculated using the Fast Fourier Transform (FFT) algorithm, which resulted in a range of main shedding frequency between 4.485 and 5.980 Hz.

In all cases, the spectral analysis produced two peaks, at 5.980 Hz and 10.465 Hz, which correspond to the main cloud and secondary cloud shedding frequency, respectively. The secondary cloud shedding frequency corresponds to a Strouhal number of 0.3 as reported by Leroux et al. [3], however the main shedding frequency obtained in the experiment was lower, around 3.5 Hz. Geng and Escaler [4] carried out a similar parametric analysis employing values from 100 to 500 and 0.02 to 0.1 for F_v and F_c, respectively, and noted that the dynamic behaviour simulated is more sensitive to the change in empirical coefficients when the cavity length is shorter. Thus, the substantial cavity length being simulated ($0.7c$ to $0.8c$) may be one reason why F_v and F_c do not significantly affect the values of f obtained in this cavitation regime. Geng and Escaler [4] took f as the response variable for their parametric analysis and found the optimal ranges of F_v and F_c to be from 300 to 500 and 0.08 to 0.1, respectively, for the cavitation regimes defined by $1.55 < \sigma < 1.9$.

The empirical coefficient study revealed that an increase in F_v from 50 to 450 resulted in an increase in V_{cav} of 18.6% and 16.9% for the SST k-ω and k-ε RNG models, respectively. The enhanced development of cavitation on the suction surface produced an increase in C_L by 5.6% and 9.2%, as well as an increase in C_D by 5% and 12.9% for the SST k-ω and k-ε RNG models, respectively. Conversely, an increase in F_c from 0.01 to 0.09 did not affect C_L or C_D, which may be explained by the fact that bubble collapse (and hence, condensation) occurs beyond the trailing edge of the foil. For this study, the optimal F_v and F_c values cannot be chosen on the basis of f since the results for this

cavitation regime are so similar. Therefore, accurate V_{cav}, C_L and C_D data is required for comparison with the simulation results and to properly extract the optimal range of empirical coefficients for the cavitation regime defined by $\sigma = 1$.

6. Conclusion

Unsteady cavitating flow around a two-dimensional hydrofoil was simulated using the Zwart cavitation model and the effects of mesh and timestep resolution, turbulence model, and the empirical coefficients F_v and F_c were investigated. The cloud cavitation dynamics was well predicted by the two URANS turbulence models modified with the Reboud correction, which produced results in agreement with experimental observations except for the primary cloud shedding frequency.

The study found that for this cavitation regime, increasing F_v led to a substantial increase in V_{cav} and hence in C_L and C_D for both turbulence models, while a change in F_c had a less significant effect on the results. Moreover, the turbulence model did not considerably affect the results obtained from the empirical coefficient study. The presented work has been supported through the collaborative programme of the VENTuRE (project no. 856887) EU funded H2020 project.

References

[1] R. E. Bensow, "Simulation of the unsteady cavitation on the the Delft Twist11 foil using RANS, DES and LES," in *Second International Symposium on Marine Propulsors*, Hamburg, Germany, 2011.

[2] J. L. Reboud, B. Stutz and O. Coutier, "Two phase flow structure of cavitation: experiment and modelling of unsteady effects," in *3rd International Symposium on Cavitation*, Grenoble, France, 1998.

[3] J.-B. Leroux, O. Coutier-Delgosha and J. A. Astolfi, "A joint experimental and numerical study of mechanisms associated to instability of partial cavitation on two-dimensional hydrofoil," *Physics of Fluids*, vol. 17, pp. 1-20, 2005.

[4] L. Geng and X. Escaler, "Assessment of RANS turbulence models and Zwart cavitation model empirical coefficients for the simulation of unsteady cloud cavitation," *Engineering Applications of Computational Fluid Mechanics*, vol. 14, no. 1, pp. 151-167, 2020.

[5] L. Zhou and Z. Wang, "Numerical Simulation of Cavitation Around a Hydrofoil and Evaluation of a RNG k-E Model," *Journal of Fluids Engineering*, vol. 130, pp. 1-7, 2008.

[6] O. Coutier-Delgosha, J. L. Reboud and Y. Delannoy, "Numerical simulation of the unsteady behaviour of cavitating flows," *International Journal for Numerical Methods in Fluids*, vol. 42, pp. 527-548, 2003.

[7] E. Goncalves, "Numerical Study of Unsteady Turbulent Cavitating Flows," Elsevier, 2010.

[8] X. Zhang, W. Zhang, J. Chen, L. Qiu and D. Sun, "Validation of dynamic cavitation model for unsteady cavitating flow on NACA66," *Science China - Technological Sciences*, vol. 57, no. 4, pp. 819-827, 2014.

[9] J. W. Lindau, R. F. Kunz, D. A. Boger, D. R. Stinebring and H. J. Gibeling, "High Reynolds Number, Unsteady, Multiphase CFD Modeling of Cavitating Flows," *Journal of Fluids Engineering*, vol. 124, pp. 607-616, 2002.

[10] J.-B. Leroux, J. A. Astolfi and B. Jean-Yves, "An Experimental Investigation of Partial Cavitation on a Two-Dimensional Hydrofoil," in *Fourth International Symposium on Cavitation*, Pasadena, 2001.

[11] I. B. Celik, U. Ghia, P. J. Roache, C. J. Freitas, H. Coleman and P. E. Raad, "Procedure for Estimation and Reporting of Uncertainty Due to Discretization in CFD Applications," *Journal of Fluids Engineering*, vol. 130, pp. 1-4, 2008.

[12] Y. T. Shen and P. E. Dimotakis, "The Influence of Surface Cavitation on Hydrodynamic Forces," in *22nd American Towing Tank Conference*, St. John's, Newfoundland, Canada, 1989.